Laboratory diagnostics

Radu Presura

9th International Conference on High Energy Density Laboratory Astrophysics, Tallahassee, Florida, April 30, 2012

Astronomical observations

- observations
- measurements from the Earth's surface
- measurements with satellites in different photon energy bands

- imaging and spectroscopy of the radiation emitted from the systems observed

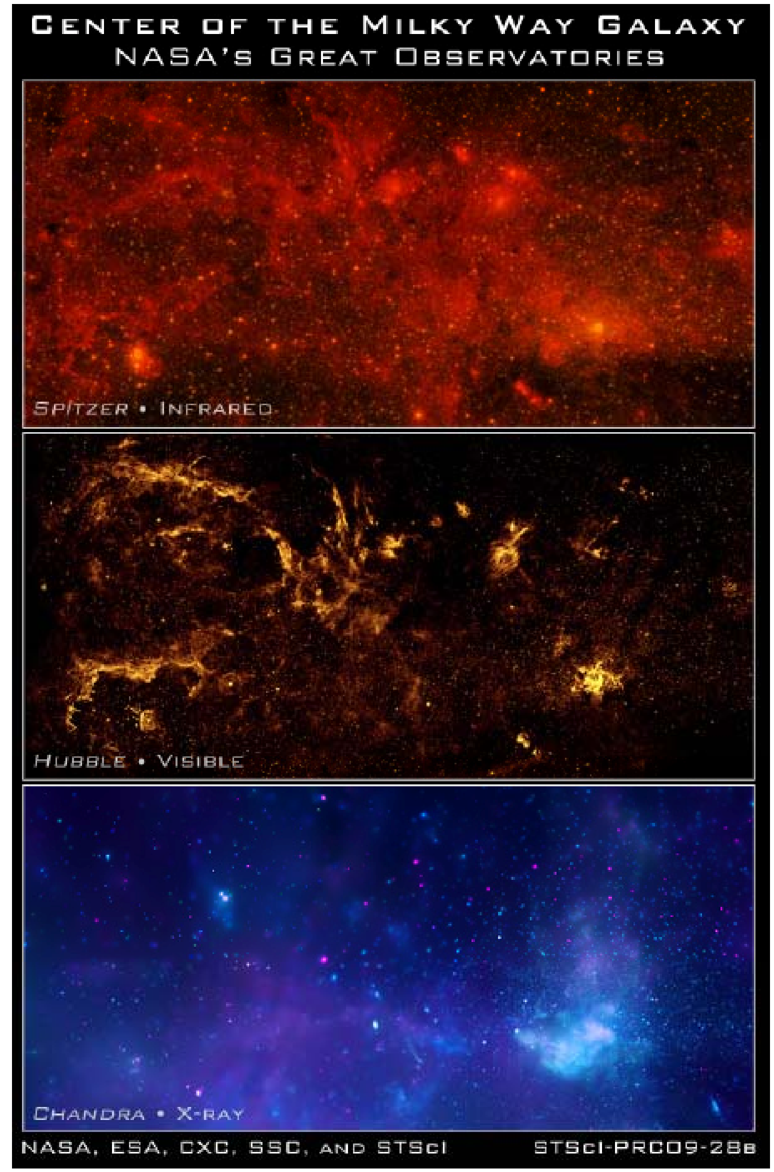

In the laboratory

- ability to simulate natural systems
  - based on scaling
  - to determine properties of matter
  - to look into details of dynamics
  - to validate theoretical models and codes

- controlled experiments are needed
  - measure radiation emitted   -passive diagnostics
  - ability to actively probe   -active diagnostics

HED Matter in the Lab and Astro

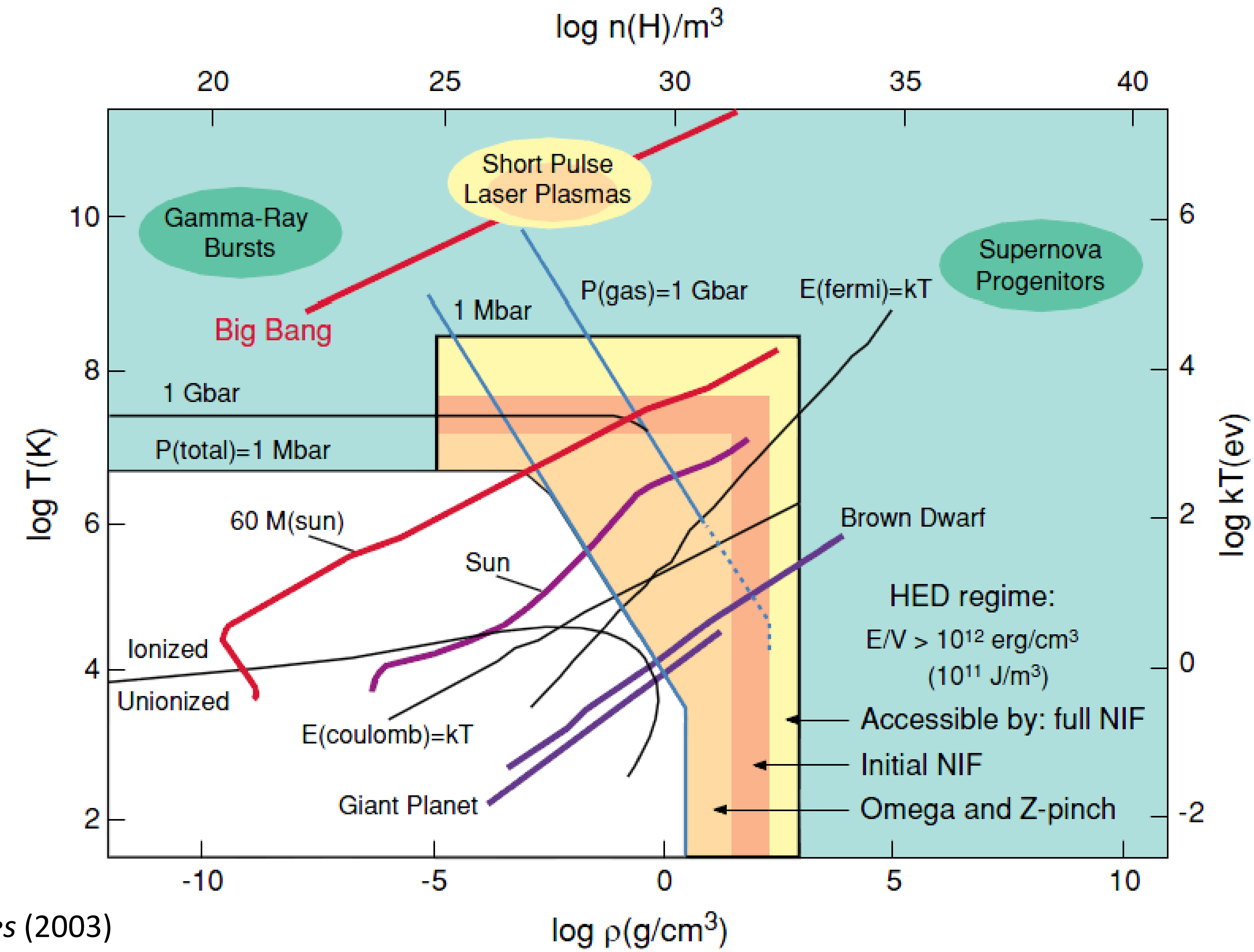

X-Games (2003)

Diagnostics

- characterize the state, structure, and dynamics of matter
- in astronomy
  - mostly imaging and spectroscopy
- in the laboratory
  - passive diagnostics
  - active diagnostics – by using an active probe
    - to improve control on the experimental conditions
      - to extend the information that can be obtained
      - in certain conditions, the properties of interest cannot be accessed through passive diagnostics

Spectroscopy

- isolated atomic system (ion)
  - ion charge
  - energy levels
  - radiative transition probabilities
- plasma: interactions with electrons, photons, ions
  - ionization – recombination → populations of ionization stages
  - excitation – de-excitation → level populations
  - spectral structure of radiative transitions
- spectrum components
  - free-free (bremsstrahlung)
  - free-bound (recombination)
  - bound-bound (line)

Spectroscopy

- spectrum features
  - continuum shape
  - line intensities
  - line profiles
  - line wavelengths

- allow the determination of
  - T_e ← line or continuum intensities
  - T_i ← Doppler broadening of spectral lines
  - n_e, n_i ← absolute intensity and Stark broadening
  - v ← Doppler shift of spectral lines
  - anisotropy ← spectral lines splitting or shift

Spectrally resolved x-ray images of inertial confinement fusion cores

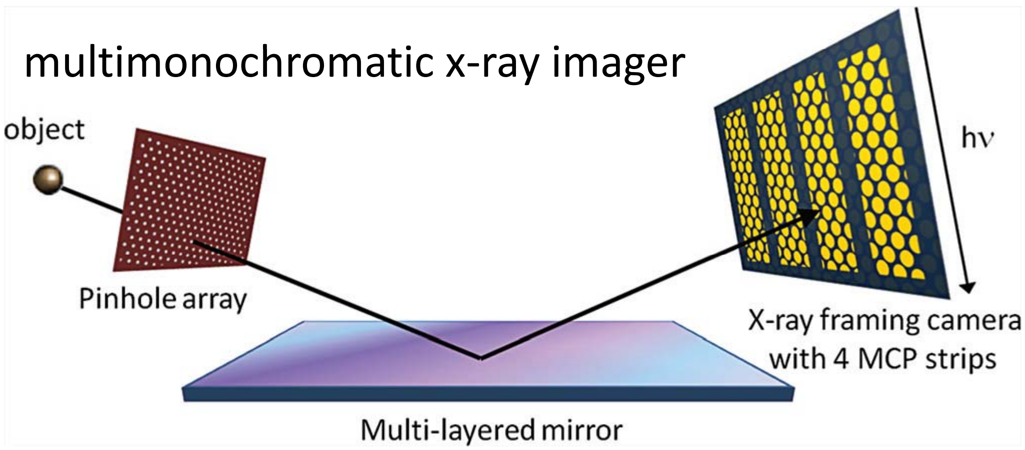

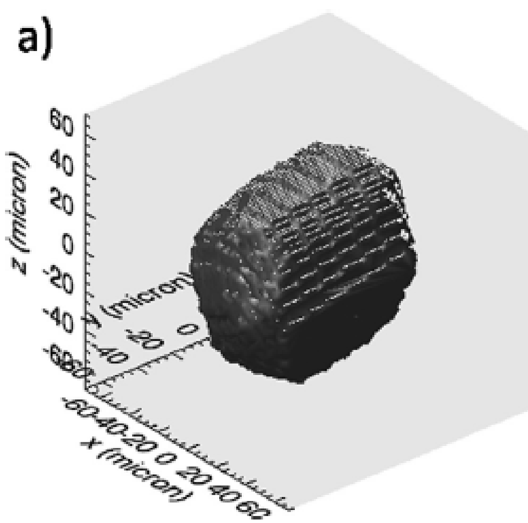

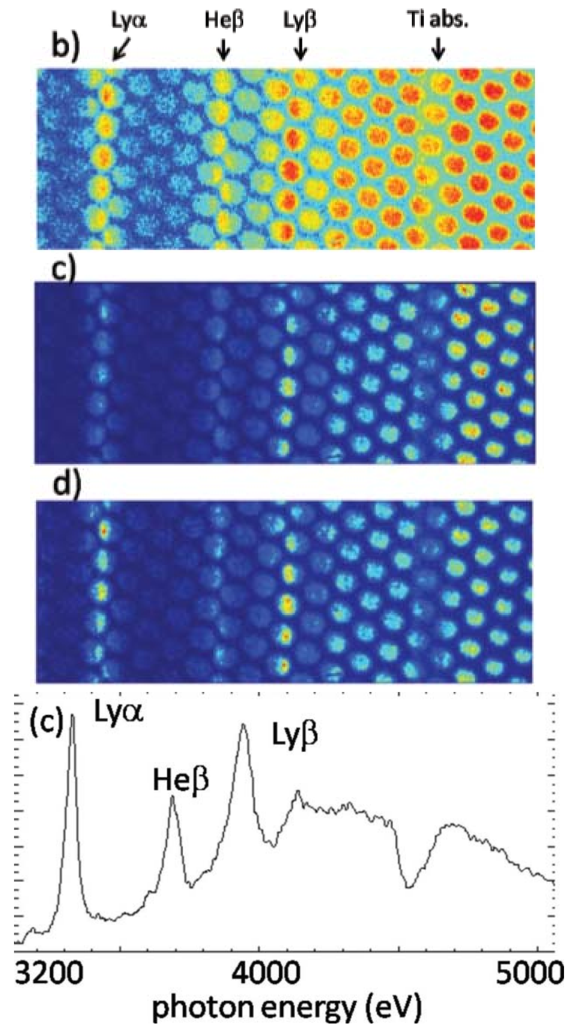

T. Nagayama *et al*., J. Appl. Phys. **109**, 093303 (2011)

Zeeman effect

- In the presence of a magnetic field, the $(2J + 1)$-fold degeneracy of each level is removed
  - Each level is split into a set of $2J + 1$ sublevels with different energies

$$\Delta E = M\, g\, \mu_B\, B$$

    - Each spectral line is split into a number of components with different wavelengths

$$\Delta\lambda_Z\,(\text{Å}) = (M_2\, g_2 - M_1\, g_1)\,(\lambda/\text{Å})^2\; 4.668\text{x}10^{-13}\; B\,(\text{G})$$

    - The selection rule for the magnetic quantum number is $\Delta M = 0, \pm 1$
    - The radiation is polarized, depending on the direction of observation

	$\Delta M = 0$ (π)	$\Delta M = \pm 1$ (σ)	sensitive to
transverse ($\perp$***B***)	linear $\parallel$***B***	linear $\perp$***B***	$\lvert \boldsymbol{B} \rvert$
longitudinal ($\parallel$***B***)	no emission	circular	***B***

Spectroscopic determination of the magnetic field distribution

-gas-puff z-pinch (320 kA, 1.6 μs peak I)
-observed along axis with radial space resolution
(⊥B, so both polarizations observed)

Line profiles dominated by Stark broadening.

-measure FWHM
-calculate the Zeeman splitting of the Stark broadened line profiles
(with B and FWHM parameters)

OIV 3s-3p (3063.5 Å)

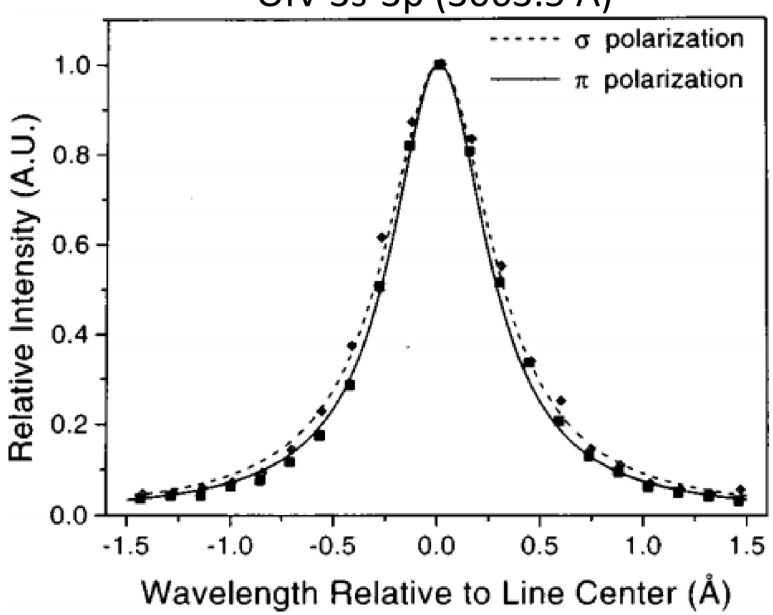

$B_\theta = 1.8 \pm 0.3$ T
$n_e = 5 \pm 1.5\text{x}10^{17}$ cm^{-3}

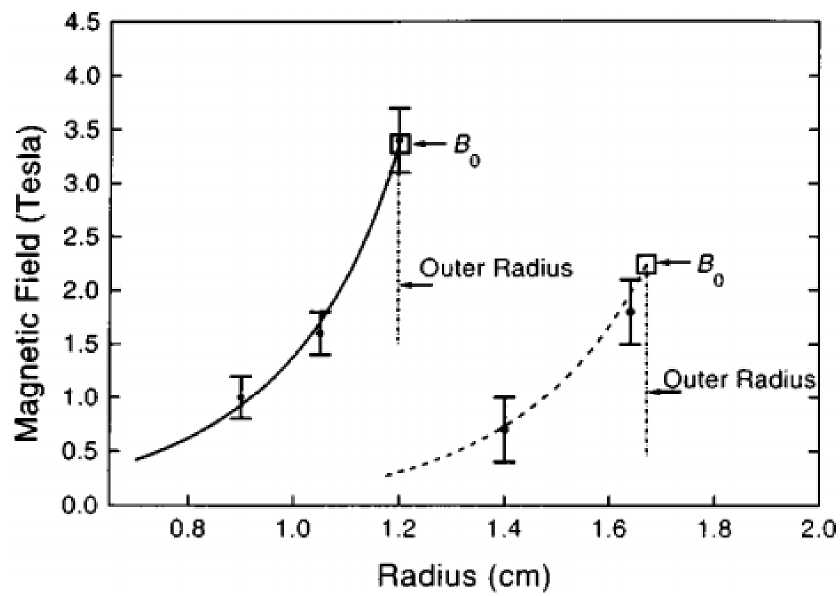

G. Davara *et al*., Phys. Plasmas **5**, 1068-1075 (1998)

Opacity

- If the radiation mean free path becomes shorter than the plasma dimensions, one must consider the radiation transport
- Transmission of radiation through matter:

$$T \equiv I \,/\, I_0 = \exp(-d/\lambda) = \exp(-\kappa d) = \exp(-\mu \rho d)$$

  - I, I_0 – the transmitted and incident intensity
  - d – path length through plasma
  - λ (cm) – mean free path (inverse of linear attenuation coefficient)
  - κ (cm^{-1}) = $\mu\rho$ – **opacity** (or linear attenuation coefficient)
  - μ (cm^2/g) – mass attenuation coefficient
  - ρ (g/cm^3) – mass density
  - $\tau \equiv -\ln(I \,/\, I_0) = \mu\rho d = d/\lambda$ **optical depth** (or optical thickness)

- the exponent is generally an integral over the radiation path
- $\kappa = \kappa\ (h\nu)$ due to the structure of the bound electron energy states
- $\kappa = \kappa\ (n_e, T_e)$ - bound energy structure depends on the ionization state

Absorption

- self-absorption limits the applicability of the spectroscopic techniques
- use an external probe and analyze its transmission through the system
  - absorption imaging
    (also called radiography or backlighting)
    - qualitative – investigate the dynamics of the system
    - quantitative – measure the density
  - absorption spectroscopy
    - quantitative – ionization state and density
- concern – radiation emitted by the target

Iron-Plasma Transmission Measured at Temperatures Above 150 eV

Opacity measurement:

1.measure the backlighter spectrum without sample
2.measure the transmitted spectrum through the sample
3.compute the transmission (the ratio of spectra)
4.determine the opacity (knowing *ρx*)

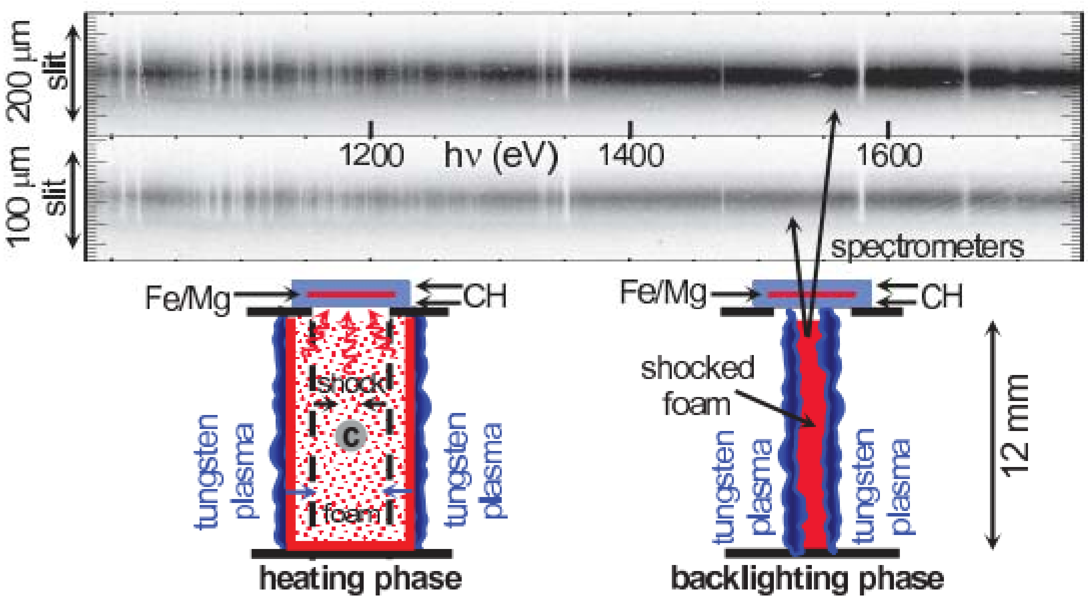

samples: Fe/Mg mixture
fully tamped on both sides by 10µm-thick parylene-N (CH)

Z-Powered Z-Pinch Dynamic Hohlraum
$T_{sample} \approx 200$ eV
$T_{backlighter} > 300$ eV (~0.5 mm, ~1–3 ns)
with almost featureless spectrum

J. E. Bailey *et al*., Phys. Rev. Lett. **99**, 265002 (2007).

Iron-Plasma Transmission Measured at Temperatures Above 150 eV

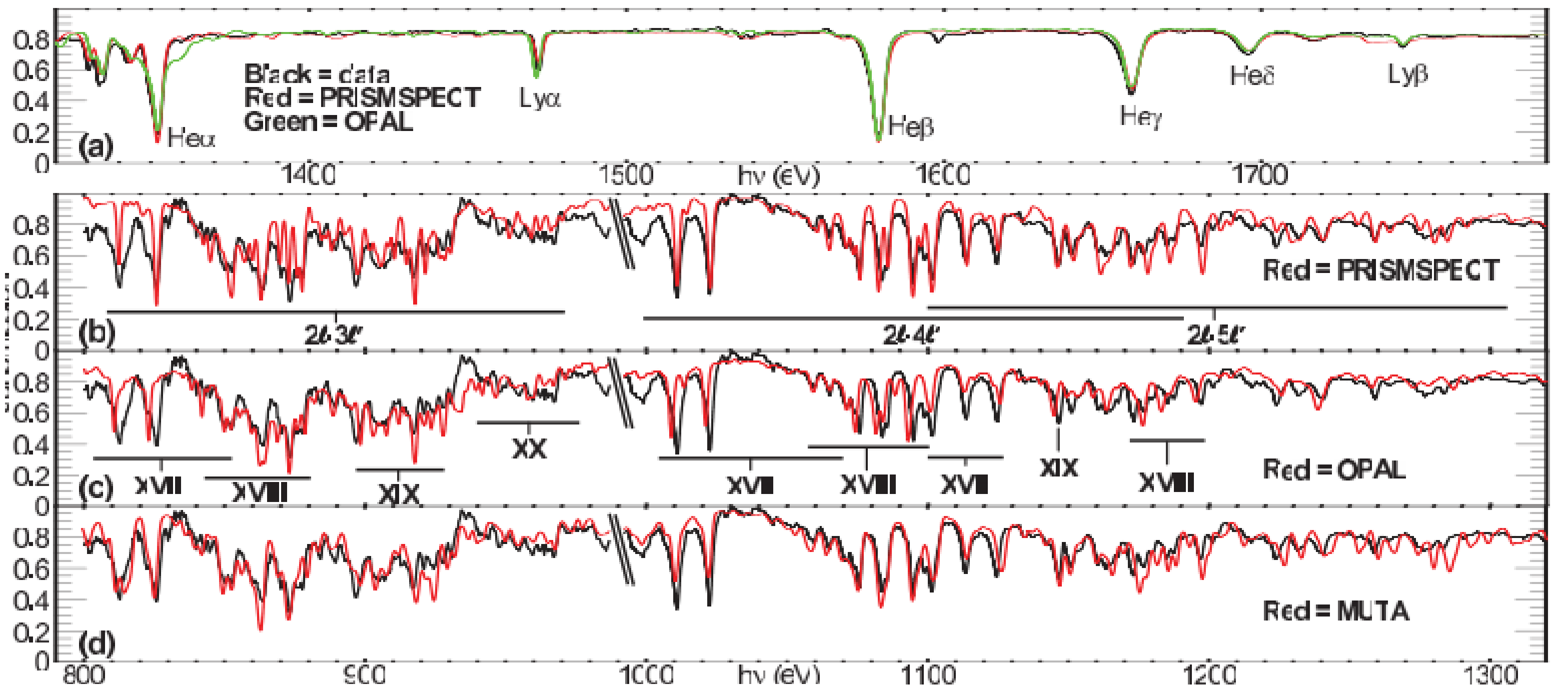

Average experimental transmission

(a) Fe b-f and Mg K shell spectra
(b)-(d) Fe L shell spectrum

Mg spectrum – to determine plasma conditions
-density from Stark broadened profiles
-temperature from relative strengths of Mg lines
LTE assumed.

T_e and n_e varied within 1σ and best agreement with the Fe b-b transitions was found at
T_e = 150 eV and n_e = 8.6 × 10^{21} cm^{-3}.

J. E. Bailey *et al*., Phys. Rev. Lett. **99**, 265002 (2007).

Quantitative X-Ray Radiography – Density Measurement

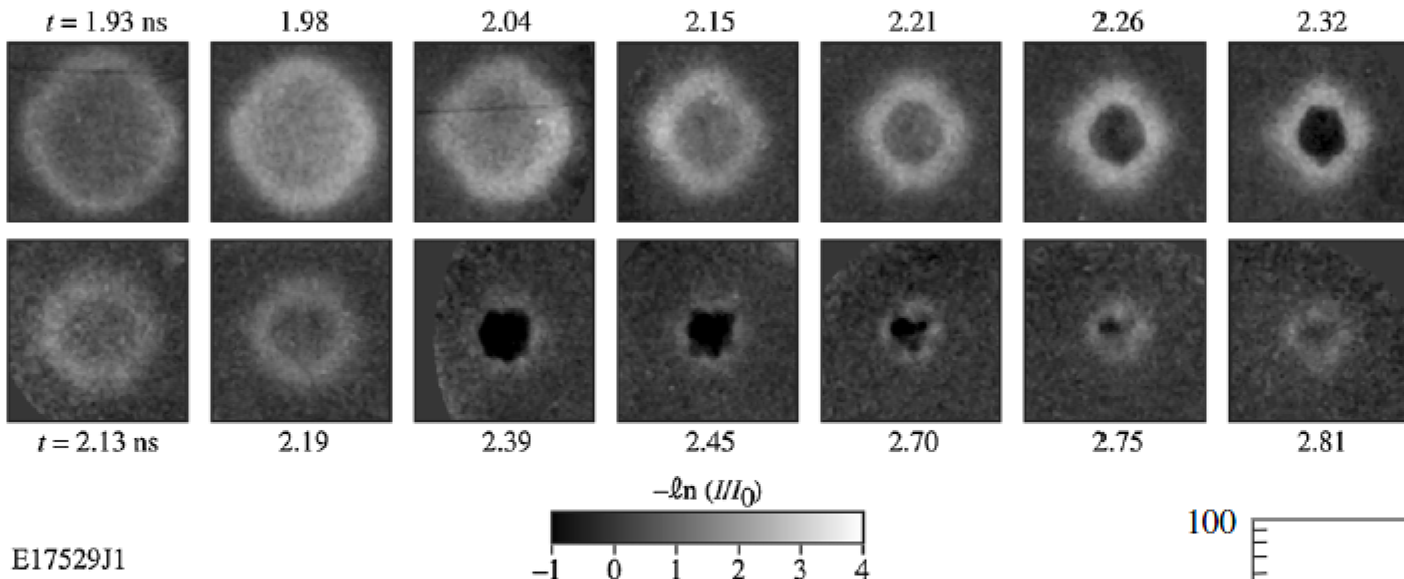

Au (~2.5 to 4.5 keV)

Ti (~4.75 keV)

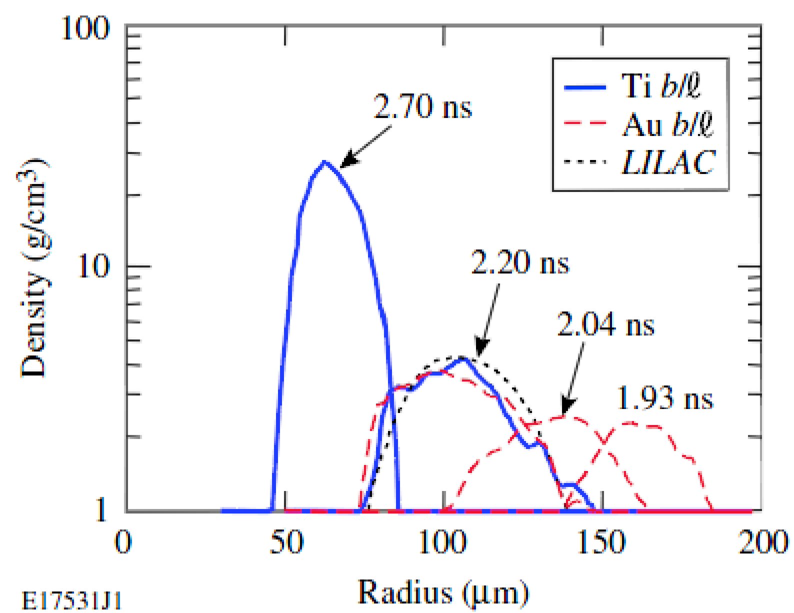

For energy bands where the absorption varies slowly: $\mu(E) \approx$ const = μ_{eff} (averaged over the energy band), so

$\rho(r) = \kappa(E,r)/\mu_{eff}(E)$.

If the total mass (of the plasma shell in this case) is known, then ρ can be determined from

$M_{shell} = \int \rho(r)\, dV = 4\pi \int dr\ \ r^2\, \kappa(E,r)/\mu_{eff}(E)$.

F. J. Marshall *et al*., Phys. Rev. Lett. **102**, 185004 (2009)

X-Ray Backlighting of the Kelvin-Helmholtz instability

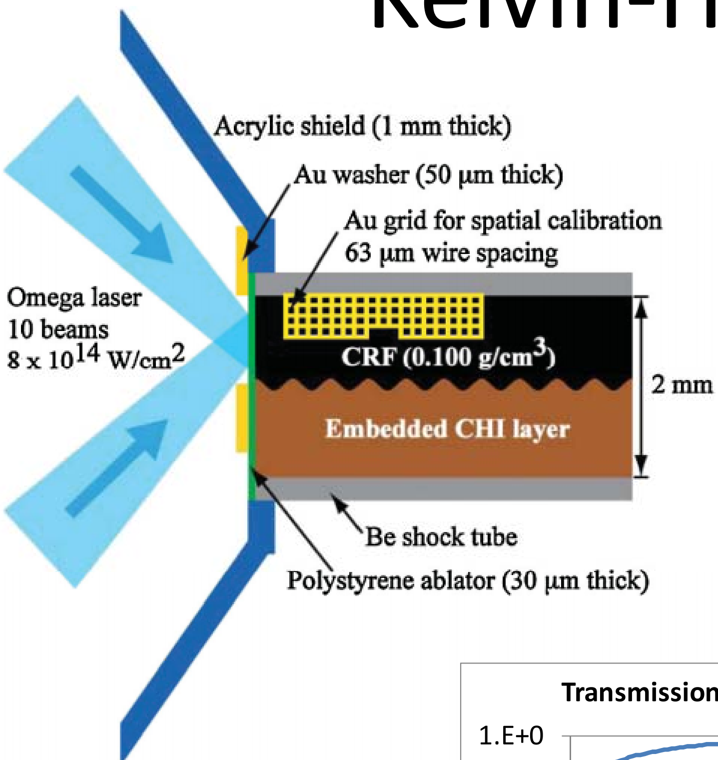

low Z system →
3% I tracer and
V backlighter, He-α 5.18 keV;
maintains low density
required for experiment
-quantitative information
about the system dynamics –
instability growth

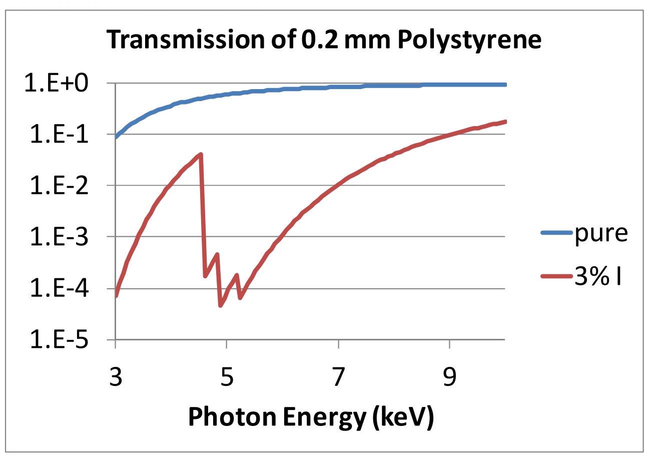

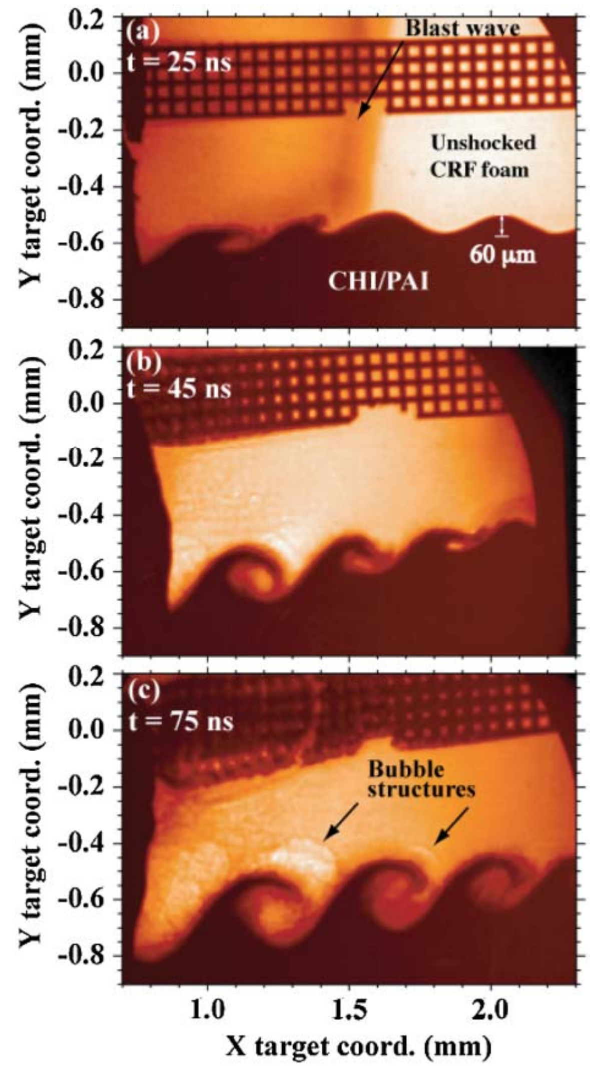

E. C. Harding *et al.*, Phys. Rev. Lett. **103**, 045005 (2009)

Other Radiation-Matter Interactions of Interest for Diagnostics

- Radiation that does not excite or ionize the matter it traverses presents additional diagnostics opportunities:
    - absorption by interaction with free electrons - inverse bremsstrahlung
    - refraction (delay and deflection)
    - scattering on free and bound electrons: Thomson, Rayleigh

Laser Refractometric Diagnostics

$$\mu = \left(1 - \frac{\omega_{pe}^2}{\omega^2 (1 \pm \omega_{ce}/\omega)(1 + i\nu_{ei}/\omega)}\right)^{1/2} \approx 1 - \frac{1}{2}\frac{\omega_{pe}^2}{\omega^2}\left(1 \mp \frac{\omega_{ce}}{\omega}\right)\left(1 - i\frac{\nu_{ei}}{\omega}\right)$$

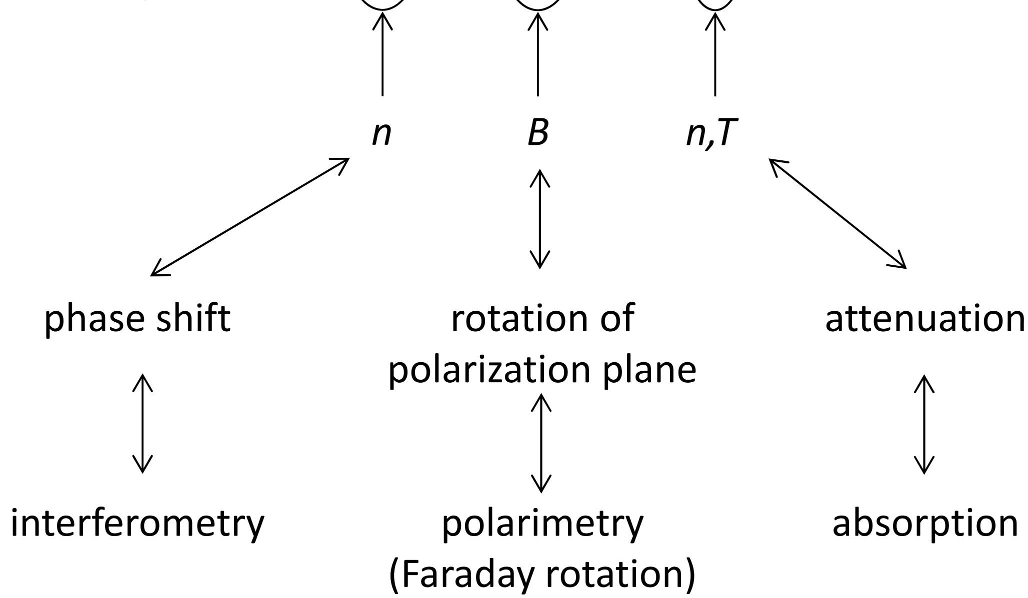

ω - laser frequency

μ - refraction index

ω_{pe} - plasma frequency

ω_{ce} - gyrofrequency

ν_{ei} - collision frequency

Internal Structure of the Dense Z Pinch

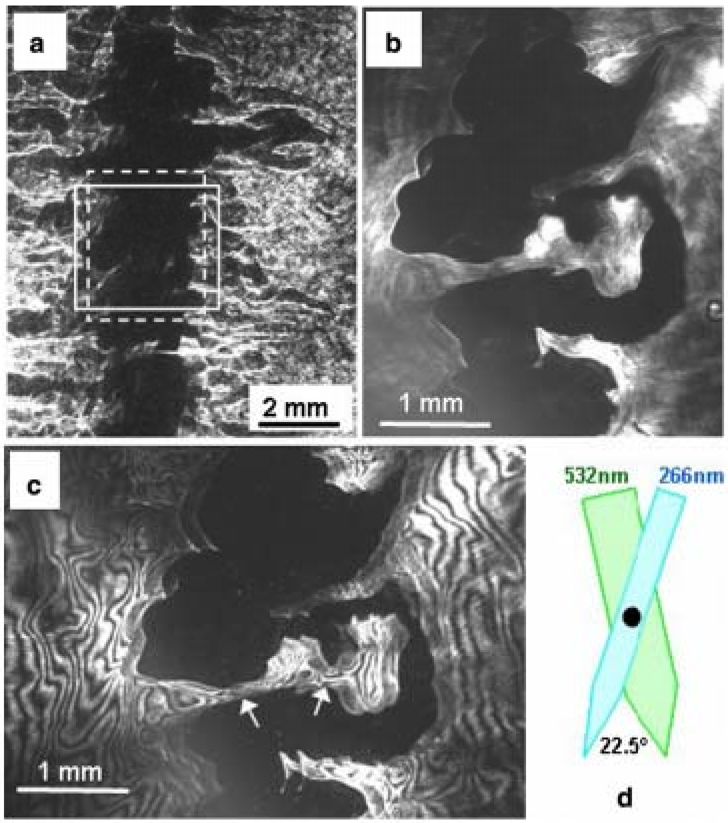

Shadow laser diagnostics
0.2 ns, 50 mJ
a: 532 nm
b,c: 266 nm ($n_c \approx 1.6\times10^{22}$ cm^{-3} ~ 100 n_{pinch})
-absorption and refraction are significantly smaller

-central part of the pinch at 0.8 ns after x-ray peak

cylindrical 16 wire array 8 mm diameter,
54 µg/cm at 1 MA

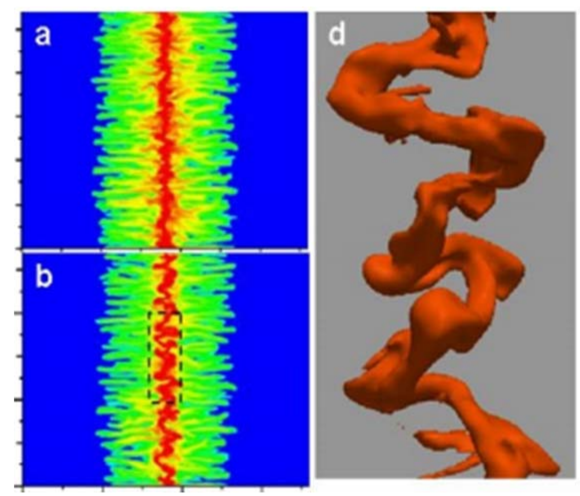

3D MHD GORGON simulation
-mass integrated along the line of sight
d) surface of constant electron density 10^{21} cm^{-3}

V. V. Ivanov et al., Phys. Rev. Lett. **107**, 165002 (2011)

Schlieren Imaging of a Blast Wave

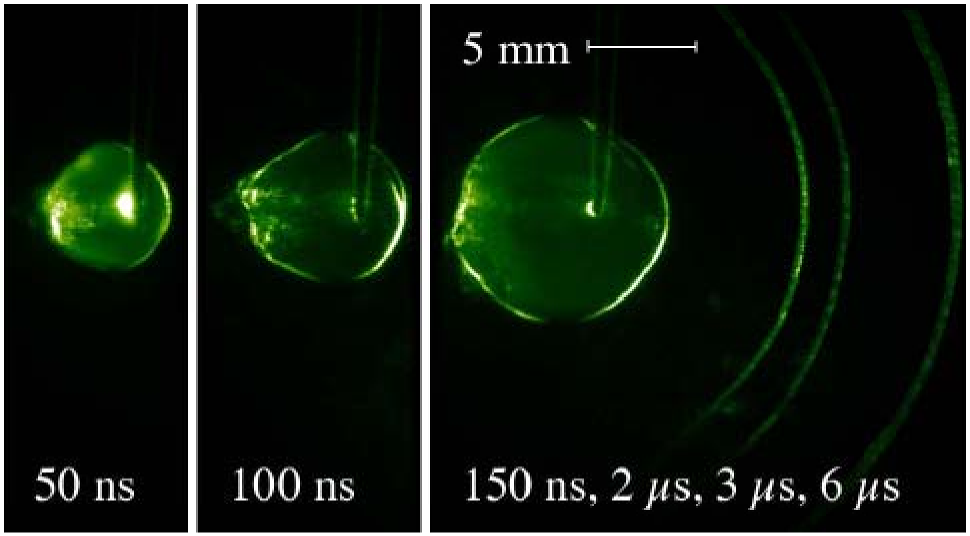

Stainless steel pin ablated with E_L = 10 J, τ_L = 5 ns laser pulse from left in 1.3 kPa ambient N_2 gas.

Schlieren set-up:
-532 nm, 15 ns laser & 2 ns gated CCD
-0.5 mm beam block - image brightness corresponds to the spatial derivative of plasma electron density.
The image to the right (t = 150 ns to 6 μs) is a composite of four images (with overlapping pin locations).

The shock is spherical and its growth is consistent with a Sedov-Taylor blast wave.

J. F. Hansen *et al*., UCRL-JRNL-155811 (Dec. 2003)

Interferometry

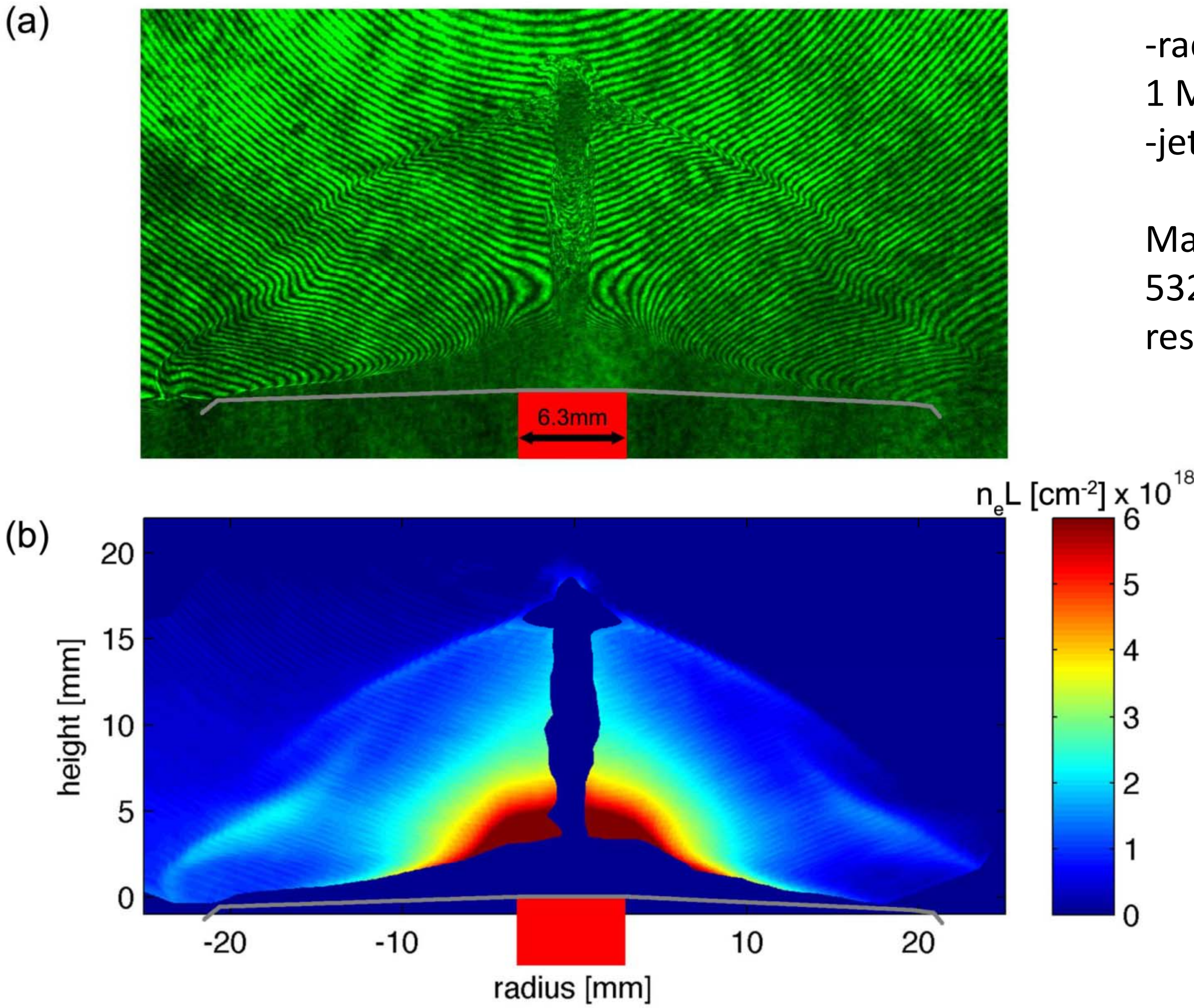

-radial foil (Al, 6-15 µm) driven by 1 MA, 250 ns current on MAGPIE
-jet interacting with ambient gas

Mach-Zehnder interferometer
532 nm, 0.3 ns, 60 mm
resolution (<1 µm, <1 ns)

The large spatial gradients of the electron density and turbulent plasma features, particularly inside the jet and at its tip, result in a complex fringe pattern, making the measurement of electron density difficult.

F. Suzuki-Vidal *et al*., IEEE Trans. Plasma Sci. **39**, 2830-2831 (2011)

Thomson Scattering

radiation → accelerates charge → charge radiates

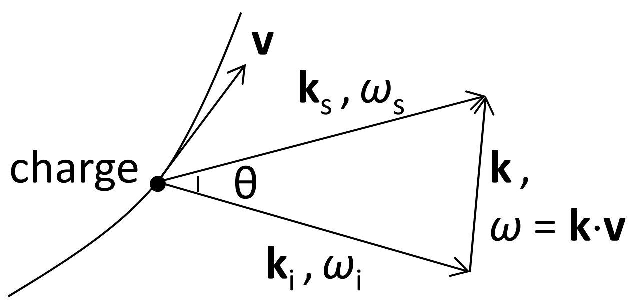

$\omega = \omega_s - \omega_i = \mathbf{k}\cdot\mathbf{v}$

$\mathbf{k} = \mathbf{k}_s - \mathbf{k}_i$

Simplifying, the scattered photons are Doppler shifted by the thermal motion of the electrons in the plasma
→ measurement of the electron velocity distribution.

Thomson Scattering

- The electrons contribute more than ions due to their smaller mass
- The incident radiation interacts with all electrons:
  - bound → elastic scattering (Rayleigh) – follow the ion motion
  - free → inelastic scattering (Thomson) – do not follow ion motion
- In the spectrum of scattered radiation:
  - ion feature
  - electron feature
- Measurements:
  - broadened Compton down-shifted feature to determine
    - electron density (from amplitude)
    - electron temperature (from width)
  - intensity ratio of the electron to ion features is a measure of the ionization balance (defined as free to bound electron density ratio)

Thomson Scattering

- The correlation of scattering charges can be described with the parameter

$$\alpha = 1/k\lambda_s\ ,$$

- $k = |\, \boldsymbol{k_i} - \boldsymbol{k_s} \,|$ and
- λ_s = correlation length, the distance over which the electrostatic forces are screened (*e.g*. Debye length of the Thomas-Fermi length)
- when
  - $\alpha \ll 1$: the scattering is sensitive to distances shorter than the screening length; the scattering charges are randomly distributed – **incoherent (non-collective) scattering** – measure of the electron velocity distribution
  - $\alpha \geq 1$: the scattering integrates over an electron and its screening particles – **coherent (collective) scattering** – spectrum depends on the collective behavior of groups of charges (e.g. at the electron plasma frequency and $\omega \approx \omega_{pe}$ and ion acoustic resonance $\omega \approx \omega_{ac}$)

Parameters of counter-streaming plasma flows

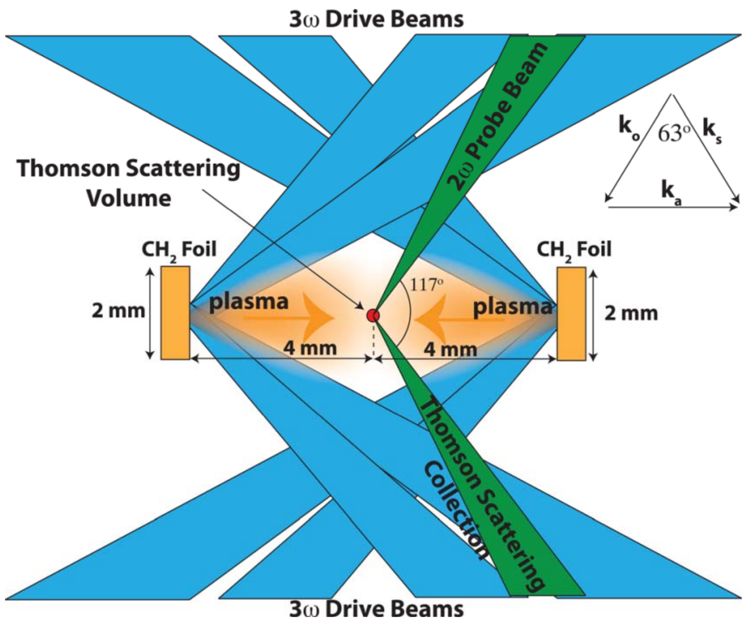

k-vector normal to the target surface

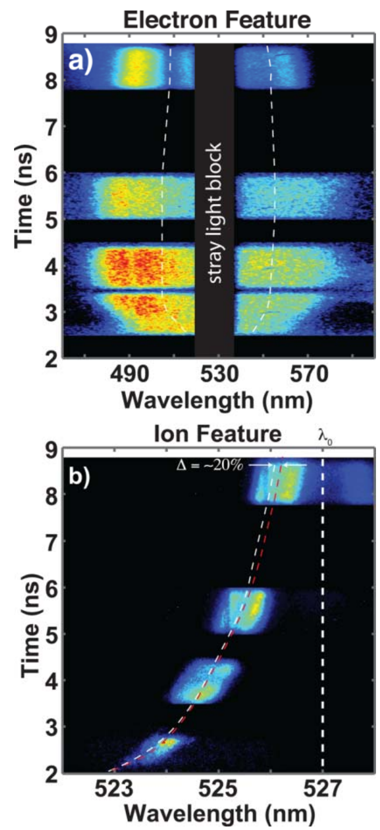

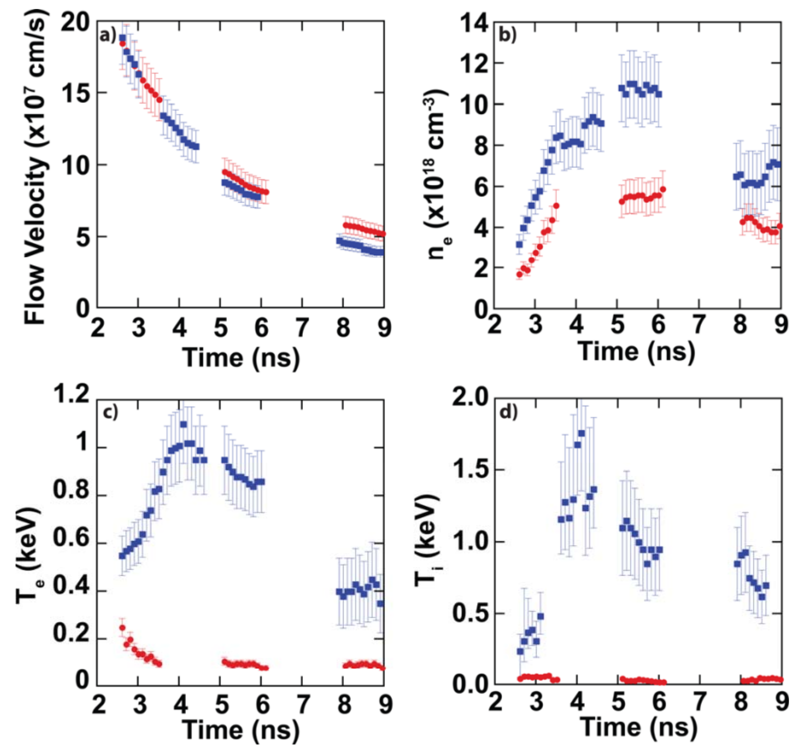

ion feature → ion temperature and flow velocity
electron feature → electron temperature, density

J. S. Ross *et al.*, Phys. Plasmas **19**, 056501 (2012)

Demonstration of spectrally resolved x-ray scattering in dense plasmas

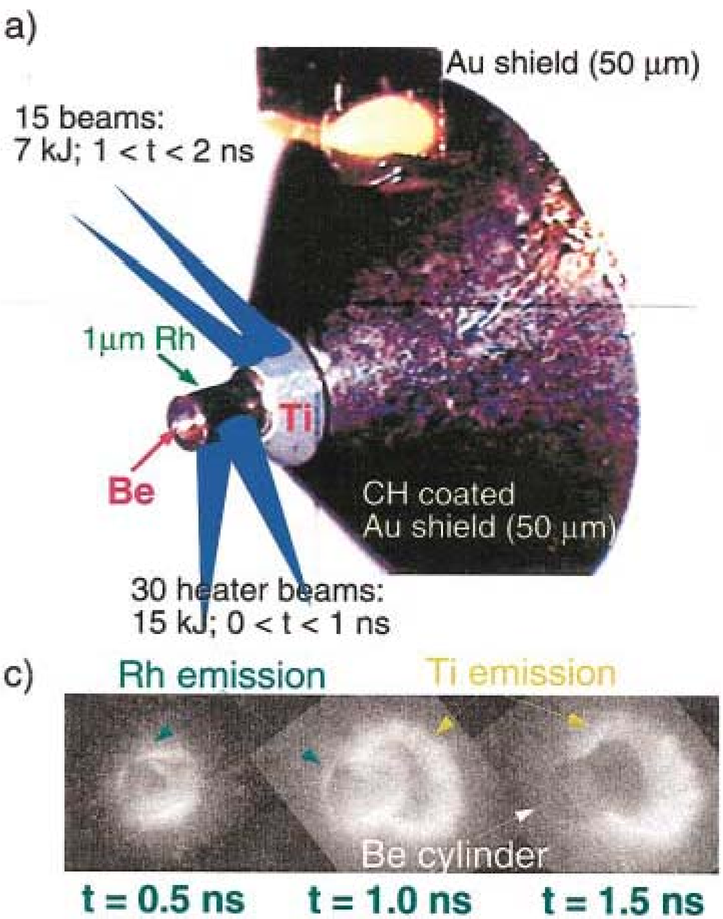

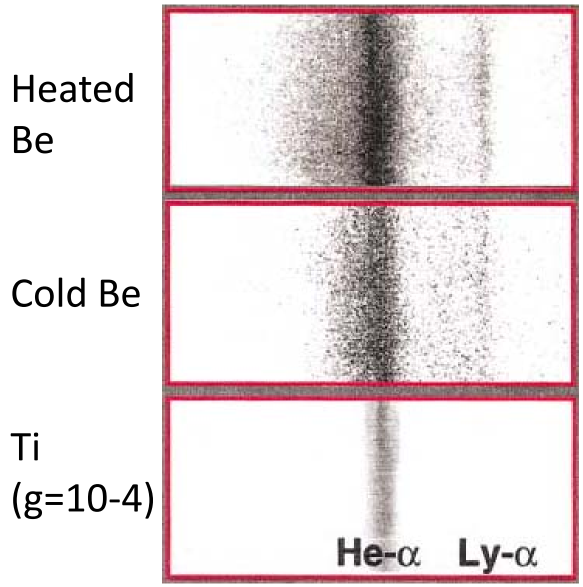

0.4 ns gate @ 1.3 ns

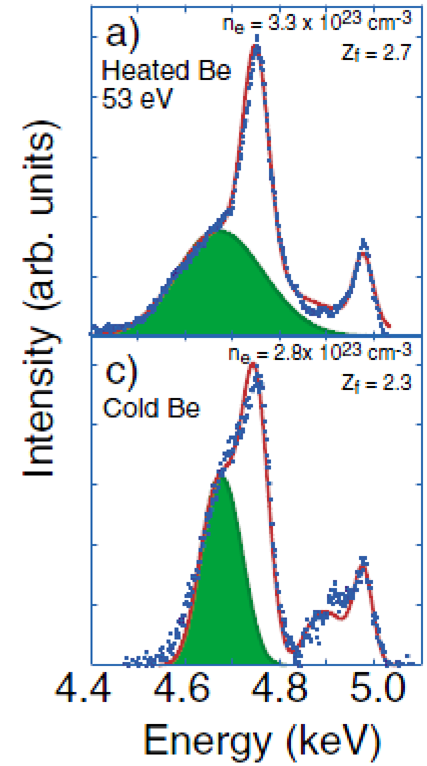

incoherent scattering

S. H. Glenzer, *et al*., Phys. Rev. Lett. **90**, 175002 (2003)

Protons as active probes

- energetic protons crossing matter suffer
  - energy loss
    areal density (radiography)

$$-dE/dx \propto n$$

  - trajectory deflection
    electric and magnetic fields (deflectometry)

$$m_p \boldsymbol{a} = \mathrm{e}\,(\boldsymbol{E} + \boldsymbol{v} \times \boldsymbol{B})$$

Density measurement with non-monoenergetic proton radiography

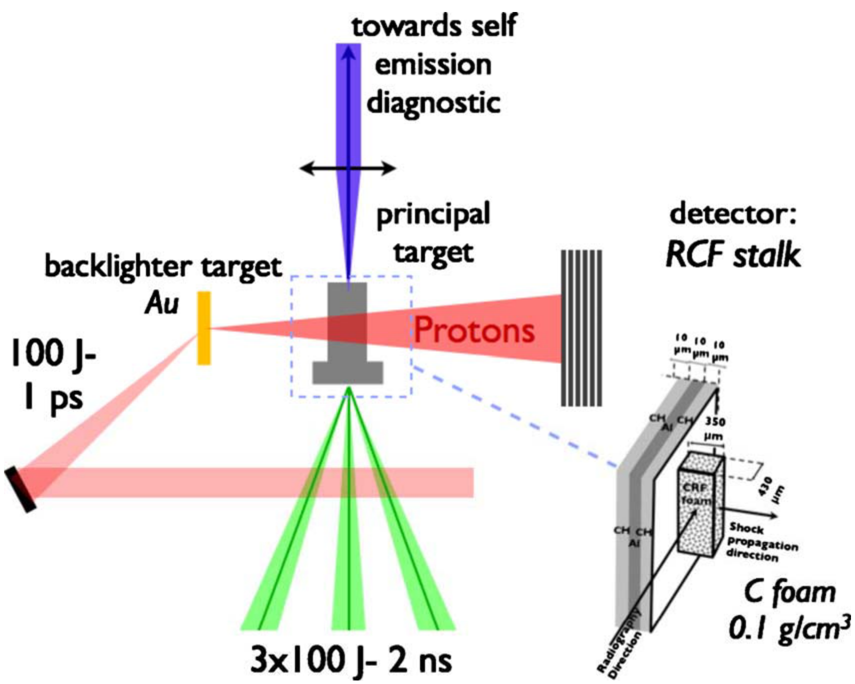

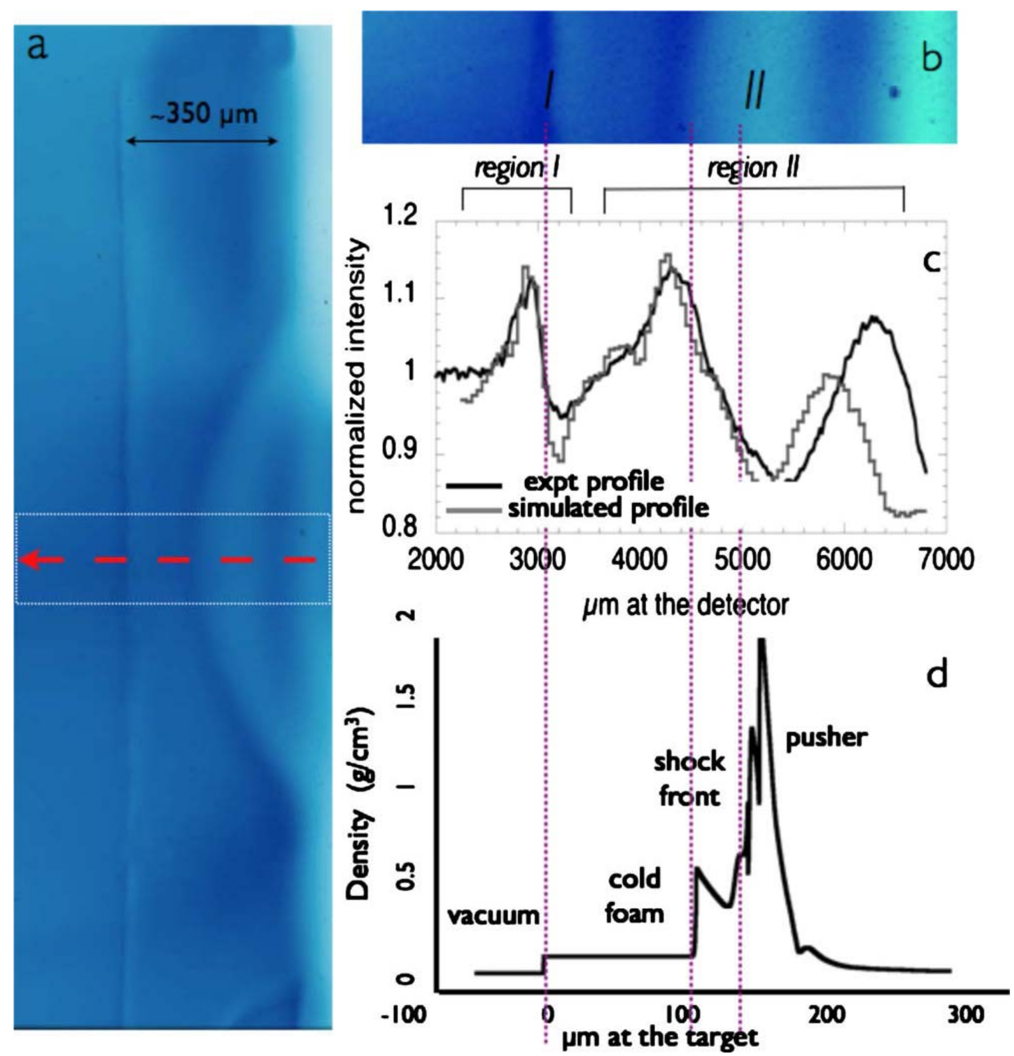

A. Ravasio *et al*., Phys. Rev. E. **82**, 016407 (2010)

Electric fields driving the laser acceleration of multi-MeV protons

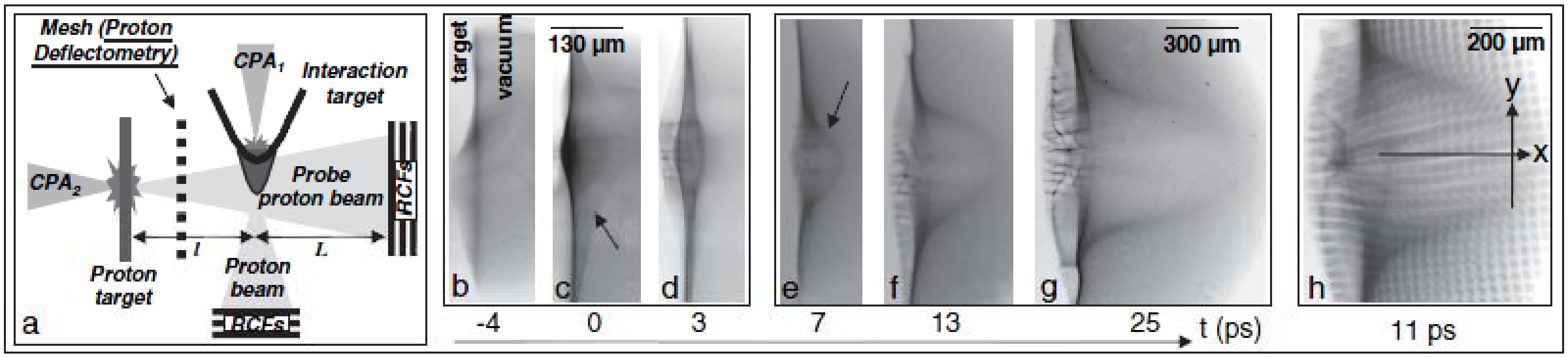

interaction target: 3.5x10^{18} W/cm^2
proton target, 10 µm Au: 2x10^{19} W/cm^2

$E_{max} \sim 3\text{x}10^{10}$ V/m

Detector: radiochromic film (RCF) stack –
intrinsic multiframe capability with temporal resolution in the range 1-10 ps.

L. Romagnani *et al*., Phys. Rev. Lett. **95**, 195001 (2005)

Proton radiography of inertial fusion implosions

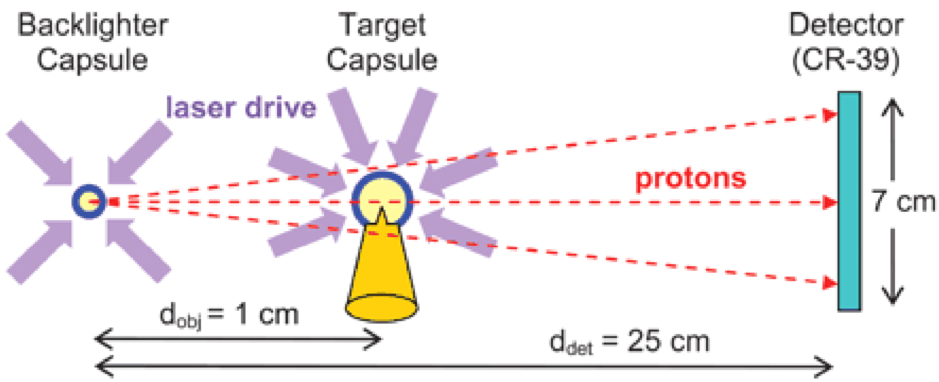

Quasi-isotropic, monoenergetic 15 MeV D^3He fusion protons from a 45 μm source.

spatial distribution of proton fluence is indicative of field structure

downshift in proton energy is proportional to the areal density

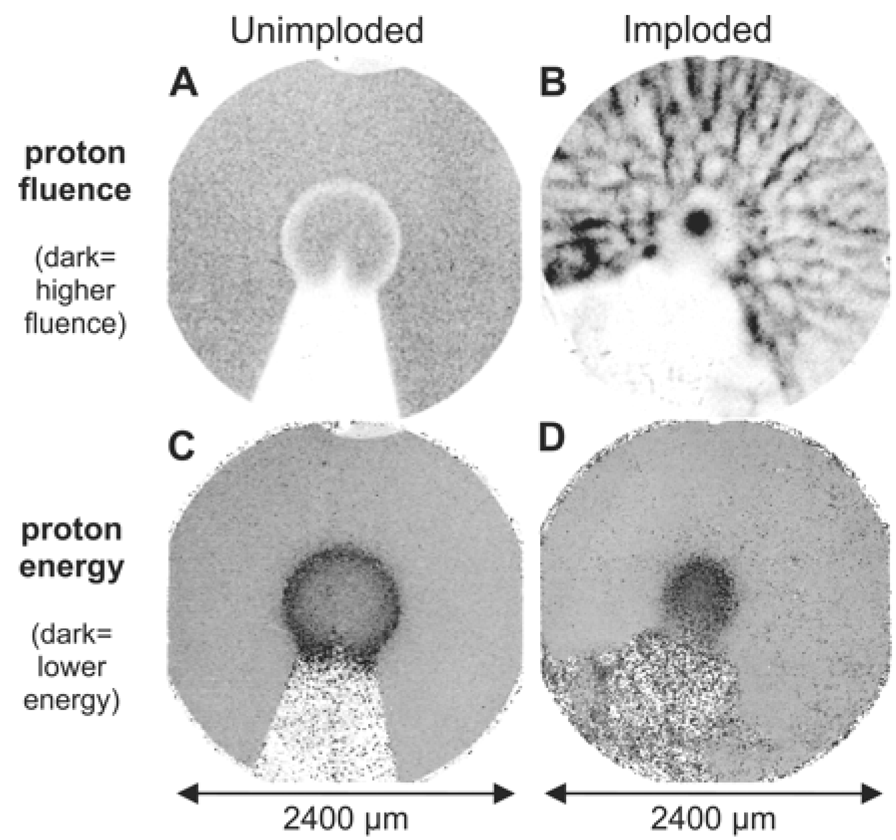

J. R. Rygg, *et al.*, Science **319**, 1223-1225 (2008)

Diagnostics applicability in (n,T) space

- Hot plasma
  - emission spectroscopy
  - refractometry
  - Thomson scattering – optical probe
- Warm dense matter
  - x-ray Thomson scattering
  - x-ray radiography
  - absorption spectroscopy
  - proton radiography

HED Laboratory Diagnostics

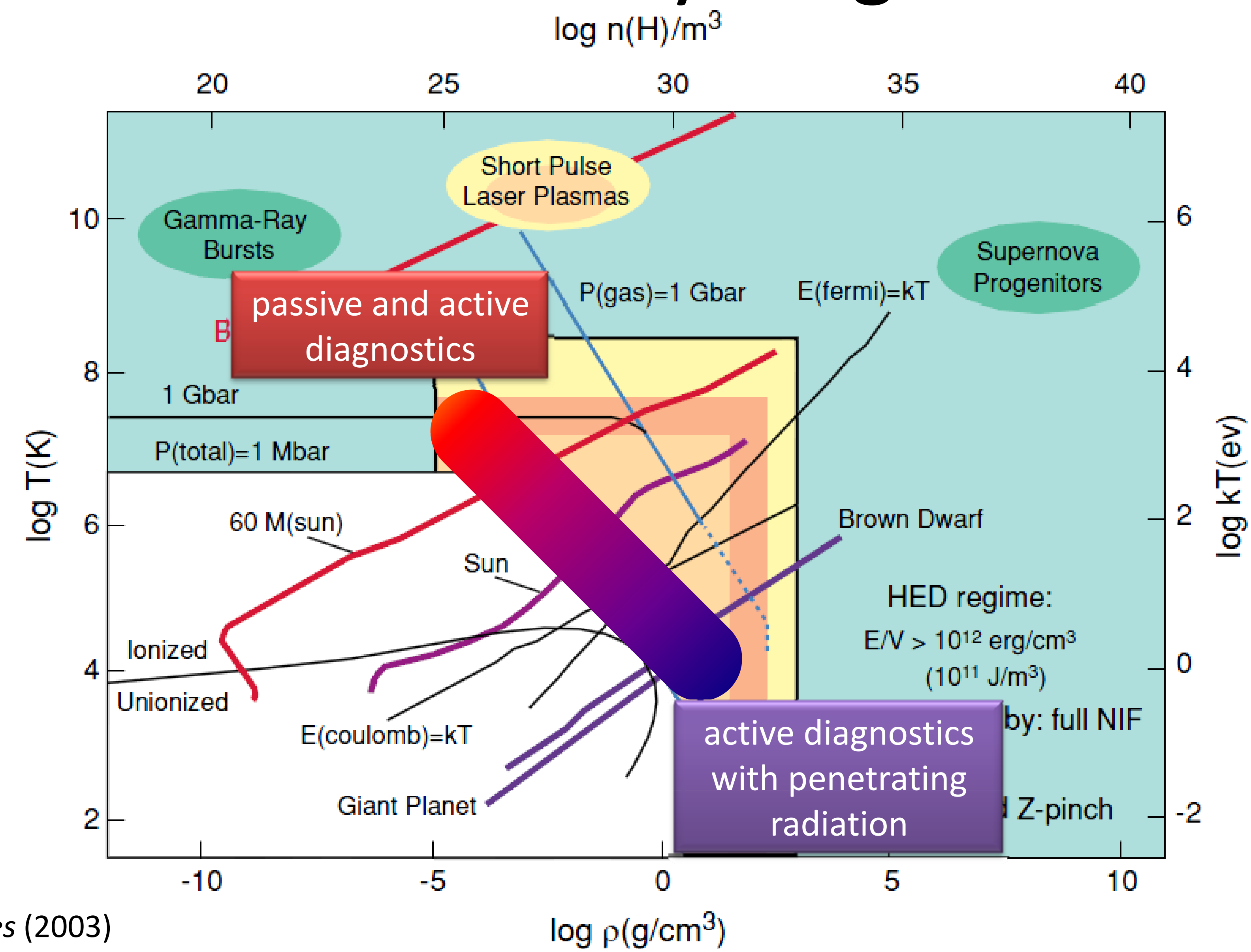

X-Games (2003)

Classification - table

technique / parameter	spectroscopy	scattering	refractometry	x-ray probe	proton probe
ρ (ni)				radiography	radiography
ne	intensity, Stark width	✓	interference	Stark abs	
Z	✓	✓		abs spectrosc	
Te	intensity, conti slope	✓			
Ti	Doppler width	✓			
B	Zeeman, polarimetry		Faraday rotation		deflectometry
E	Stark shift				deflectometry
v	$v_{\|\|}$ Doppler	✓	$v_{\perp}$ multiframe	$v_{\perp}$ multiframe	$v_{\perp}$ polyenerg

Magnetic Field Diagnostics

	p deflectometry	**Magnetic probes**	**Zeeman splitting**	**Faraday rotation**	**Pulsed polarimetry**
B in plasma	yes	no	yes	yes	yes
B projection	$\perp$ (proton path)	$\vert\vert$ (loop axis)	$\vert\vert$ (sightline)	$\vert\vert$ (sightline)	$\vert\vert$ (sightline)
Active	Proton beam	NA	No (self-emission)	Lin. polarized light	Lin. polarized light
Time resolution	Energy spread	yes	with gated det.	Laser pulse τ	yes
Sightline space resolution	Possible (forward modeling)	Local measurement	no	no	yes
Lateral space resolution			yes	yes	no
Sensitivity to other plasma parameters	E, n_i	(Plasma shielding)	n_e, n_i, T_e, T_i, $v_{\vert\vert}$	n_e, ∇n_e, δl	n_e
Sensitivity to probe parameters	energy spectrum, angle distribution	C (response time), size (averaging)	NA	Wavelength	Wavelength, pulse duration
Main advantages	Sensitive, space resolution	Very sensitive	Works at higher density; passive	Lateral resolution	Can measure alternating fields
Main difficulties	Scattering, electric field	Interactions with plasma, radiation	Other broadening mechanisms	Know density, depolariz. effects	Know density, fast detection
Quantity measured	$\int B_{\perp} dl$	$dB_{\vert\vert}/dt$	$\int B_{\vert\vert} dl$	$\int B_{\vert\vert} n_e dl$	$B_{\vert\vert} n_e$
Minimum B measurable	< 50 kG (10 MeV, 0.5 cm)	> 0.1 kG (literature)	< 100 kG (100 eV, 10^{19} cm^{-3})	>1 50 kG (10^{19} mm/cm^3, 0.1 cm, 1064 nm)	> 100 kG (5×10^{19} mm/cm^3, 0.02 cm, 1064 nm)

How to chose the best diagnostics?

- define (and prioritize) the **observables** for the experiment – passive / active diagnostics?
- estimate the **value ranges** for the main parameters – passive / active diagnostics?
- take into account the **facility capabilities** diagnostics already in place or probe availability
- take into account the **theoretical and modeling support** available (does the analysis involve intensive modeling or postprocessing?)
- take into account the **personnel** available manageable number of techniques
- take into account the **time available** is it a good time to try new diagnostics?

- → the best diagnostics are at the intersection of all these conditions